

# Analysis of Stress Concentration Factor for Tensile Characteristics of Syntactic Foam Using Finite Element Method

Zulzamri Salleh<sup>1,2</sup>, Md Mainul Islam<sup>1,\*</sup> and Jayantha Ananda Epaarachchi<sup>1</sup>

<sup>1</sup>Centre for Future Materials, Faculty of Health, Engineering and Sciences, University of Southern Queensland, Toowoomba, QLD 4350, Australia

<sup>2</sup>Universiti Kuala Lumpur, Malaysian Institute of Marine Engineering Technology, 32200, Lumut, Perak, Malaysia

**Abstract:** This paper presented the stress concentration factor (SCF) around the half circular edge of tensile specimens made of syntactic foam using finite element software Strand7 software. The study is a preliminary effort, which investigates the effect of variations of crack geometry on the stress concentration factor on a tensile specimen subjected to a constant, uniform, uniaxial tensile load. The material property is graded for varying Young's Modulus and Poisson's Ratio with different composition of glass microballoons. Finally, a uniform pressure is applied at the top and the model is constrained with symmetric boundary conditions at the left and bottom. As the result, these numerical results for both SCF experimental and simulation model are compared to those obtained from analytic fracture mechanics procedures and are found to be varied. In addition, the SCF is sensitive to the modulus of elasticity, particularly for lower composition weight percentage (wt.%), while it is also varied with the different weight percentage (wt.%) of glass microballoons, which is led by 2 wt.% specimen.

**Keywords:** Finite element analysis, Syntactic foam, Stress, Concentration, Factor, glass microballoon, resin.

## 1. INTRODUCTION

Stress concentration in panels particularly with geometrical discontinuities in the form of cut outs (various shape) and holes have received wide attention in the literature cause to the fact that they often lead to failure. Previous study proposed that the stress concentration factor (SCF) can be reduced by using the functionally graded layer [1]. For homogeneous material panels the problem has been widely studied and a number of analytical, numerical and experimental techniques are available for reduction of the stress concentration factor (SCF) around discontinuities. In Nagpal *et al.* [2] an overview of various techniques developed to reduce SCF is presented: some authors proposed, for example, removing material around the hole by using auxiliary holes or reinforcing the hole with composite material rings. Chao *et al.* [3] obtained a general solution for a reinforced elliptic hole embedded in a matrix subjected to remote uniform load. The solution, based on the technique of conformal mapping, permits one to find the optimum design of the reinforcement layer in order to reduce stress concentration and interfacial stresses. Recently, Batista [4] studied SCF for different complex geometries of holes in homogenous plates subjected to uniform loads at infinity by using a modified Muskhelishvili method.

In order to determine the SCF of an area in the panels, mainly structural analysis was implied. Nowadays, there are two type of testing, which is proposed to detect this failure mode either by destructive testing (DT) or Non-destructive testing (NDT). NDT is particularly advantageous for the preventive maintenance in structural construction, through failure analysis by using finite element analysis (FEA), and post treatment (PT) of damages [5, 6]. However, Reale *et al.* (1995) argued on whether NDT will be able to give the correct information on the defectiveness of a component and structure [6]. This prior information regarding the defective components and structures creates an appropriate platform for structural integrity assessment, obtained through the implementation of fracture mechanics approach. Ingraffea and Wawrzynek (2004) found in their research, this fracture mechanics approach can be used as a quantitative failure analysis tool for predicting the propagation and the failure of the surface of a component or structure with a pre-existing crack [7]. These fractured mechanics might begin with cracks caused either by material cracks, discontinuities in geometry or damages whilst in fabrication.

In this case, mechanical properties particularly tensile testing is required to investigate the modulus elasticity and Poisson's ratio of syntactic foam. Previous study stated that, the Poisson's ratio is dependent on the composition of the composite material is observed, highlighting the need for developing a comprehensive understanding of

\*Address correspondence to this author at the Centre for Future Materials, Faculty of Health, Engineering and Sciences, University of Southern Queensland, Toowoomba, Queensland 4350, Australia; Tel: +61 746311388; Fax: +61 746312110; E-mail: Mainul.Islam@usq.edu.au

Poisson's ratio for other engineered composites. Poveda *et al.* (2010) found that different types of glass microballoon with different sizes cause the Poisson's ratio to vary [8]. Other experimental work also showed that the modulus of epoxy or vinyl ester matrix syntactic foams can be tailored within a range of 1–3 GPa while their strength can be controlled in the range of 30–110 GPa [9, 10].

Beside of experimental work, theoretical studies also tend to assume the Poisson's ratio using the model particularly in FEA. Previous report also mentioned that lack of availability of Poisson's ratio values is a limitation for modelling efforts [11]. The determination of both the modulus of elasticity and Poisson's ratio from the experiment can be used in FEA modelling to finalise the SCF value of syntactic foam.

Desirable to composite plate subjected to various transverse static loading conditions [12]. They found, that the peak stress concentration factor occurs on the boundary of the hole and that the stress concentration factor was also strongly influenced by the uniformly distributed normal and equivalent stresses. Limitation of availability the characteristic in tensile properties such as modulus elasticity and Poisson's ratio in functional graded material like syntactic foam lead to focus in this study using the modelling FEA methodology.

This paper presents the characterisation of the tensile properties of a dog bone specimen glass microballoon/vinyl ester syntactic foam. The main objective of this work is to investigate the behaviour of syntactic foam under tensile loading by using FEA.

Tests on coupons and full-scale specimens were undertaken to determine the tensile properties of syntactic foam. The tensile tests on coupons were conducted. On the other hand, the tests on full scale specimen were performed using the procedures available in previous studies. The details of these tests are presented in the next sections. Aside from these tests, a finite element analysis (FEA) particularly stress concentration factor (SCF) was carried to simulate the tensile behaviours of full-scale specimen by using the Strand7 software. The results obtained from the experiment were compared with those of FEA.

## 2. MATERIAL AND METHOD

### 2.1. Material

The vinyl ester resin with scientific name as diglicidyl ether of bisphenol A-based resin and methyl ethyl ketone peroxide (MEKP catalyst, used as the matrix material, are procured from NOROX Australia. The glass microballoons used in this study are non-porous in nature and are manufactured and supplied by Potters Industries Inc. under the trade name of Q-CEL Spherical (R) Hollow Microspheres. In this study, the physical shape of glass microballoon has spherical glass powder typed with chemically-stable fused-borosilicate glass and non-porous microsphere. The mean inner diameter is calculated by taking the difference in the average true particle density of solid and hollow particles made up of same material. The physical properties of glass microballoon supplied by the manufacturer is given such as main glass from soda lime borosilicate with average size  $72\mu\text{m}$  (range 5- 150  $\mu\text{m}$ ), bulk density,  $\rho = 110 \text{ kg/m}^3$  and maximum working pressure 500 MPa.

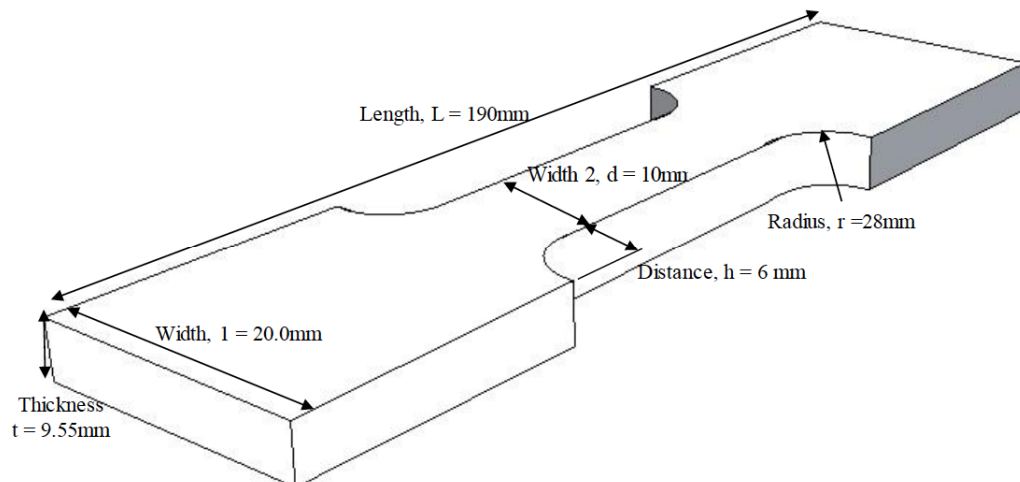


**Figure 1:** The dimension for tensile specimen with the 'dog bone' shape.

## 2.2. Fabrication of Syntactic Foam

“Dog bone” shaped steel moulds are used for preparing tensile specimens. The dimension drawing of the specimen also can be seen at Figure 1 with length = 190mm, width = 20.0mm and thickness = 9.5mm. First of all the moulds were cleaned using acetone and the surface have been coated with degreasing wax to ensure that the syntactic foams can be removed easily. The mould releasing agent was silicone gel type, especially for the stainless steel mould type similar to mention in [13].

In the literature it is found that stir mixing is the common method to fabricate the syntactic foams. Then the conventional mixer by using the glass rod is commonly used nowadays, but the stir mixer machine using stir magnetic bar as a mixer is better performer or else using the ultrasonic machine. The mixture can also be manually shaken for gelatinised the starch and microballoons in a container [14]. Conventional method needs to be followed carefully to avoid the breakage of microballoons [14]. This synthesis method consists of mixing measured quantities of glass microballoons in the resin and mixing them until slurry of uniform viscosity is obtained. The mixing time is approximately between 4 to 5 minutes. Then, the required amount of microballoons depending on the percentage was weighed separately and was added slowly to the resin mixture. Stirring time was increased for a lower volume percentage of microballoons to ensure uniform distribution of glass microballoons in the resin. As the amount of the glass microballoons increases, the viscosity also increased and the mixtures have putty like consistency.

In this study, if more contents of glass microballoons were added into vinyl ester resin such as more than 10 wt.%, the viscosity of the slurry also increased. Hence, it will make possible to stir the slurry because it became the dough and stick to each other's. Therefore, the selection of composition glass microballoons in weight percentage also is important to ensure that this phenomenon can be eliminated during sample preparation. The mixture was then transfer to a tensile stainless steel mould after smeared with silicone gel (mould releasing agent). The sample along with the mould will be allowed to cure for 24 hours at room temperature and then removed from the mould. To ensure complete curing, the sample was then post-cured at 60 – 80 °C for 4 hours in hot air oven. Similar with tensile specimen, the synthesis method for preparation the compression specimens were consists of mixing measured quantities of glass microballoons with different weight percentage (2 wt.% – 10 wt.%) were measured by using the digital weighing machine in one decimal point for accuracy purpose. Then the vinyl ester resin was weighed by using same machine and mixing them until a slurry of uniform viscosity is obtained with the intermittent mixing approximately 4 -5 minutes for each mixing. The hardener then is added into this slurry and gently mixed using a glass rod until completely mixing for approximately 4 ~ 5 minutes.

## 2.3. Experimental Method

The tensile test was performed in a 100 kN capacity MTS with model machine Insight Electro-mechanical testing machine using a crosshead speed of 1.25 mm/min. The test was conducted in accordance with standard ASTM D-638-10 [15]. An extensometer was

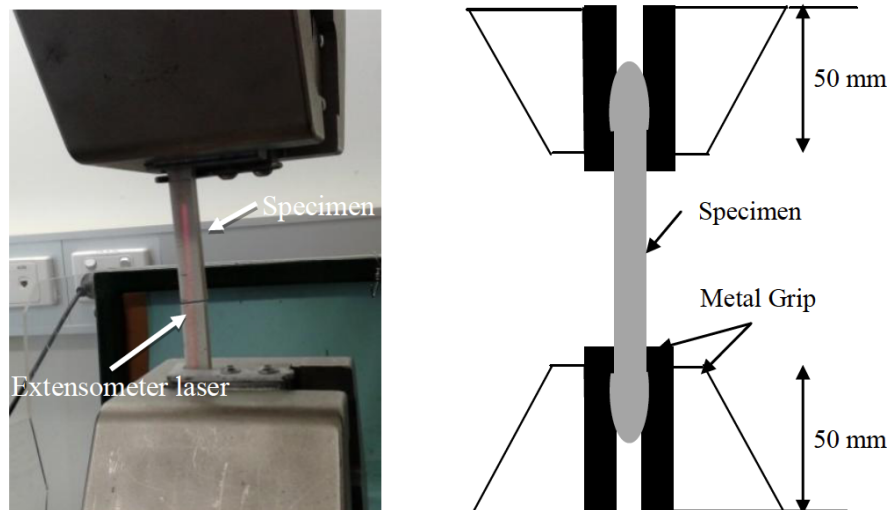


**Figure 2:** Overview of representative test set-up of coupon specimen.

used at the gauge length to measure the longitudinal and transverse deformations for determination of strength, modulus and Poisson's ratio. The experimental set-up used in conducting the tensile test is shown in Figure 2.

#### 2.4. Stress Concentration Factor (SCF)

Stress Concentration factors ( $K_t$ 's) for numerous "simple" geometries have been determined by researchers (analytical equations). Warren and Richard have compiled these into easy to use tables [16]. Determining stress concentration factors ( $K_t$ ) for complex geometries can be difficult because are highly localized effects on functions of geometry and loading. In order to predict the "actual" stress resulting from a geometric stress raiser, a theoretical stress concentration factor is applied to the nominal stress. For a part subjected to a normal stress, the true stress in the immediate neighbourhood of the geometric discontinuity is calculated as mention at Equation (1);

$$\sigma_{\max} = K_t \times \sigma_{\text{ref}} \quad (1)$$

Where  $\sigma_{\max}$  is maximum stress,  $K_t$  is stress concentration factor and  $\sigma_{\text{nom}}$  or  $\sigma_{\text{ref}}$  is nominal stress. While for  $\sigma_{\text{ref}}$  can be determined by using the Equation (2) below;

$$\sigma_{\text{ref}} = \frac{\sigma_{\infty} \times w}{w - 2h} \quad (2)$$

Equation (2) was derived based on the stress is infinite with 100MPa,  $w$  is width of specimen and  $h$  is total length including with radius semicircle to the symmetry line [17]. The dimension geometry loading for Equation (2) show at Figure 3 for details.

From the Figure 4, it is shows that the resultant stress/strain/displacement fields in each quarter will be same when it is divided by the both horizontal and

vertical symmetry lines. Therefore, it is necessary to build only one quarter strip as long as the applied force along at the edges where symmetry conditions exist to make quarter model behave in the completed strip. Similar with the geometry loading for tensile specimen. In the case of dimension geometry tensile loading shown at Figure 4 used in this study.

Timoshenkor and Goodier also found that the stress distribution in a rectangular filleted bar in simple tension obtained through photoelastic procedures was observed in their research [22]. In this study, the SCF,  $K_t$  was calculated according to Roark's formula shows at Equation (3) for details;

$$K_t = C_1 + C_2 \left( \frac{2h}{D} \right) + C_3 \left( \frac{2h}{D} \right)^2 + C_4 \left( \frac{2h}{D} \right)^3 \quad (3)$$

Where

$$C_1 = 1.006 + 1.008 \sqrt{\frac{h}{r}} - 0.044 \left( \frac{h}{r} \right), C_2 = 0.115 - 0.584 \sqrt{\frac{h}{r}} + 0.315 \left( \frac{h}{r} \right),$$

$$C_3 = 0.245 - 1.006 \sqrt{\frac{h}{r}} - 0.257 \left( \frac{h}{r} \right), C_4 = 0.135 + 0.582 \sqrt{\frac{h}{r}} - 0.017 \left( \frac{h}{r} \right)$$

for the case of  $0.1 \leq h/r \leq 2.0$ .

#### 2.5. Comparison with Elliptical Hole Modelling

Stress concentration factor also can be compared between theoretical values and numerical value which is calculated by using the equation from the under uniaxial tension stress and tensile loading. Yang *et al.* [19] introduced that the factor elliptical hole can be derived from the Equation (4)

$$K_{te} = K_t \times \sigma_{\text{ref}} \quad (4)$$

#### 2.6. Finite Element Analysis (FEA)

Generally, Finite Element Analysis (FEA) was involved in the development of the basic stress

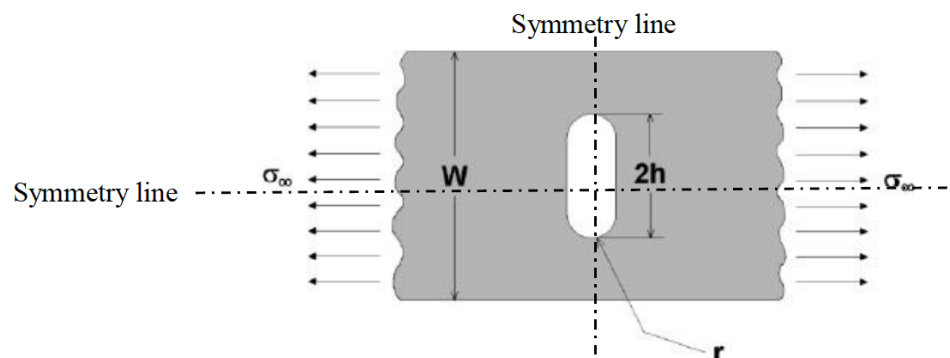
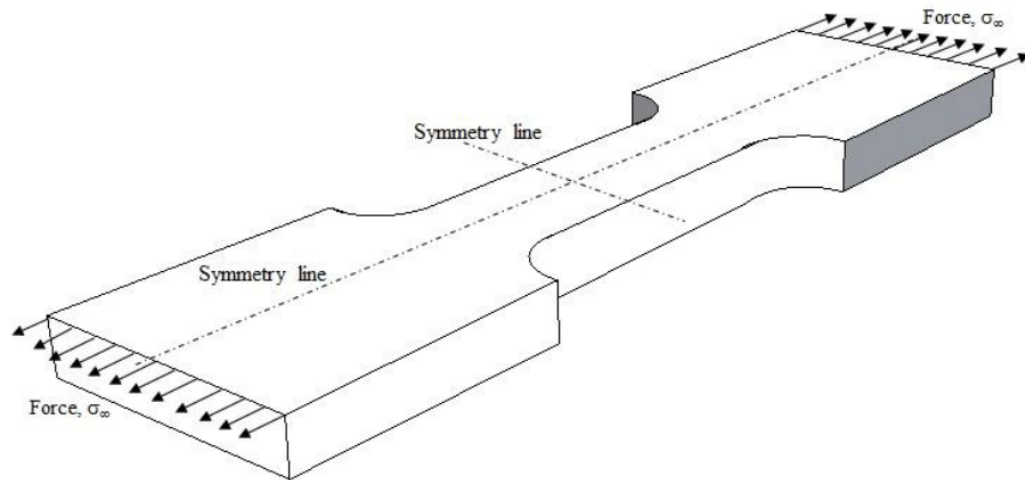


Figure 3: Schematic diagram for geometry loading of the strip [18].



**Figure 4:** Schematic diagram for geometry tensile loading of the strip.

equations for tension, compression, bending, and torsion, it was assumed that no geometric irregularities occurred in the member under consideration. Physically to implement FEA in engineering application particularly mechanical engineering may have difficulties when considered to design a machine without permitting some changes in the cross sections of the members. For example the rotating shaft must have shoulders designed on them so that the bearings can be properly seated and so that they will take thrust loads, also the shafts must have key slots machined into them for securing pulleys and gears, etc. [20]. Hence, when considering all these items, it is abrupt changes in geometry can give rise to stress values that are larger than would be expected [21]. This can be a source of difficulty for machine designers when it develops which play an important role in the design stage. In order to apply the FEA in this case let us consider, for example, the state of stress in the tension member of

two widths illustrated in tensile shape of the specimen. Spotts *et al.*, (2004) considered the stress geometry for the near each end of the bar the internal force is uniformly distributed over the cross sections [22]. The nominal stress in the right part can be found by dividing the total load by the smaller cross-sectional area, the stress in the left part can be found by dividing by the larger area. However, in the region where the width is changing, a redistribution of the force within the bar must take place. In this part, the load is no longer uniform at all points on the cross section, but the material in the neighbourhood of points B in Figure 5 is stressed considerably higher than the average value. The maximum stress occurs at some point on the fillet, as at B, and is directed parallel to the boundary at that point. By using the Strand 7 software, the stress maximum occurred at B can be investigated by using the FEA 2D model.

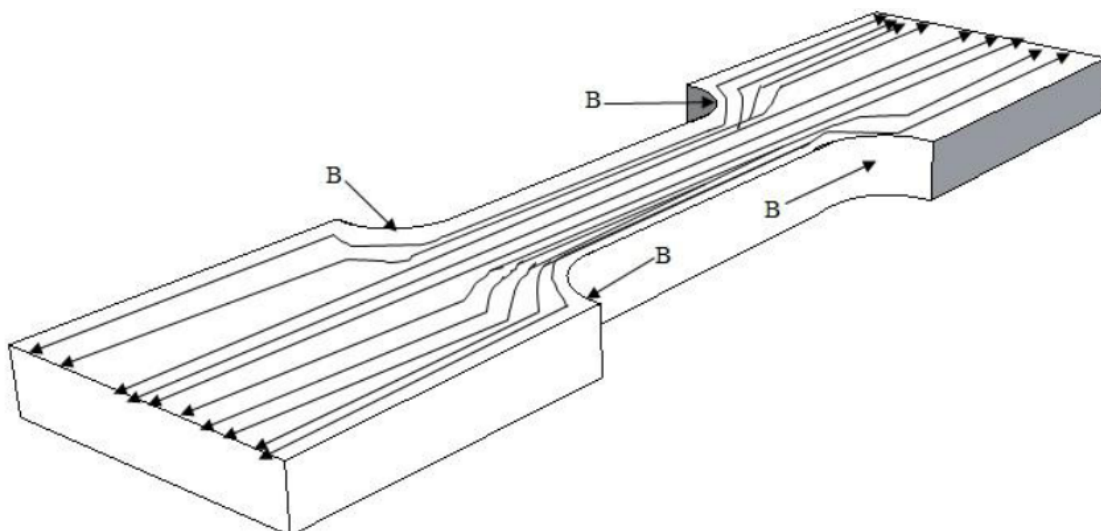


**Figure 5:** Stress distribution over the cross sectional for tensile specimen.

The quarter symmetry lines in vertical position at middle of tensile specimens for 2D FEA have been used in this study to investigate the SCF syntactic foam. The model also called as two dimensional solid model used for plane stress analysis. Darwish *et al.* (2013) used the quarter two dimensional model in order to determine stress concentration for countersunk rivet holes in orthotropic plates [23]. Pilkey and Pilkey (2008) also summarized and reported that numerous studies on the stress concentration of two dimensional (2-D) plates with circular holes subjected to several loading types [24]. While Shivakumar and Newman (1992) used 3D finite element results of the SCF were presented by for plates with circular straight-shank holes subjected to remote tension [25]. Their results showed that the maximum SCF lies at the mid-thickness of the isotropic plate and drops near the free surface. The FEA also can be performed for both isotropic and orthotropic plates as long as SCF occurred near to the holes area. Wu and Mu (2003) performed FEA on uniaxial and biaxial loaded isotropic and orthotropic plates with circular holes and examined the SCF of holes in a plate structures and pressure vessels [26]. Kotousov and Wang (2002) presented analytical solutions for (3-D) stress distribution around

typical stress concentrators in an isotropic plate of arbitrary thickness [27].

In the present study, FEA is integrated with the software called Strand 7 to determine the SCF syntactic foam material. In strand 7 the surfaces of specimen can be subdivided into element and will meshing for each of them as well. The nodes are created based on the specimen size of tensile in millimetre units. In Strand 7 work, the nodes and elements were identified according to the actual size of tensile specimens. The representative model for material property in Strand 7 is shown at Figure 6 in this study. Then the subdivide section have been used to refine the mesh of the quarter size of tensile specimen before it was given the force at edge area. The total of nodes is 70 nodes and plate elements are 47 plates have been used in this study.

The colour contour in meshing of the element representative the stress distribution occurred in the tensile specimen can be shown in Figure 7 for details. From the contour, the red colour is representative for the higher stress distribution while the light blue colour is representative for the lower stress distribution. The rest of the colour is moderate which is between the

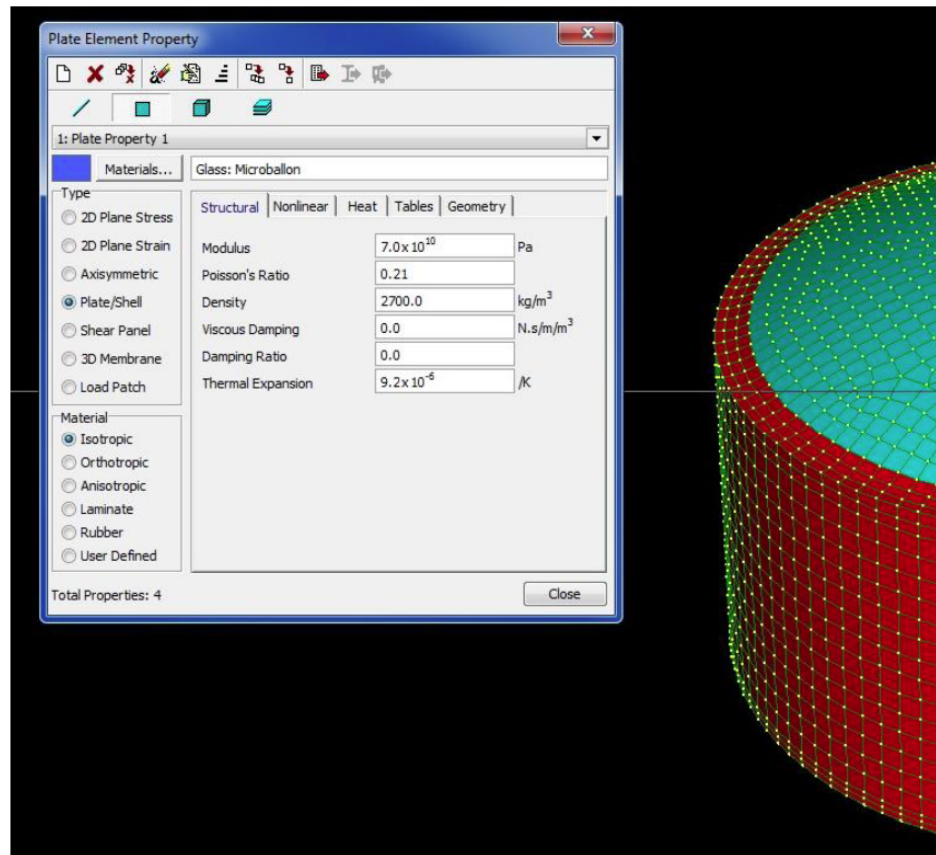


**Figure 6:** Material property for plate element used for modelling FEA in Strand 7.

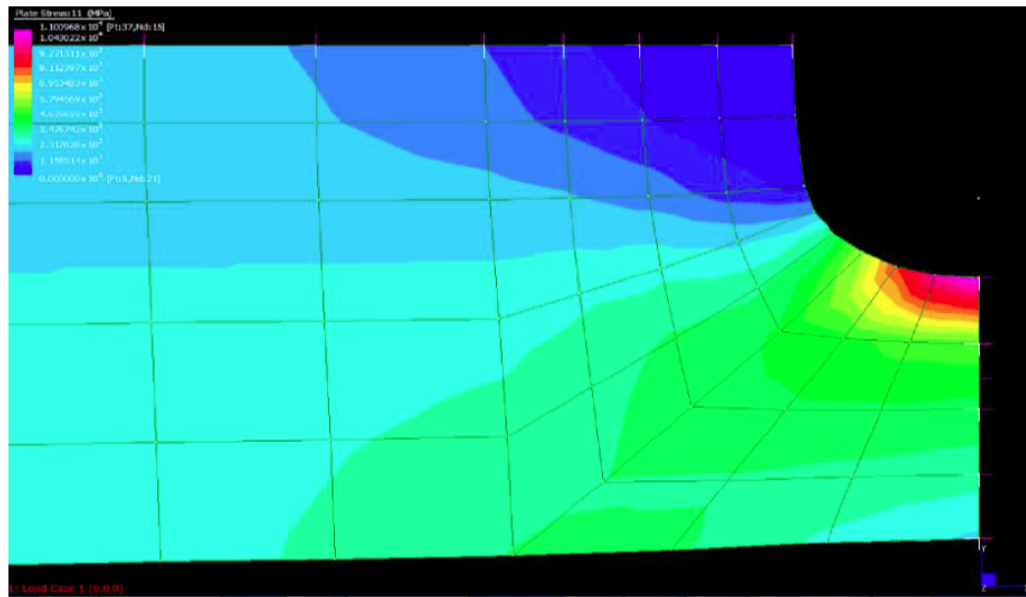


**Figure 7:** The representative of 2D stress distribution for the tensile specimen.

higher and lower stress distribution area. The maximum stress,  $\sigma_{\max}$  from the FEA which is located at red colour area can be used for the calculation of SCF in this study. The SCF for experimental and calculation in FEA can be compared and error can be determined to ensure the accuracy of the experimental values.

### 3. RESULTS AND DISCUSSION

#### 3.1. Tensile Property

The tensile property of the vinyl ester/glass microballoon syntactic foam for different composition of glass microballoon contents has been carried out. The specimens were indicated their name as SCFT-01, SCFT-02, SCFT-03, SCFT-04 and SCFT-05. The representative stress–strain curves for vinyl ester/glass microballoon syntactic foam specimens are presented in Figure 8. These curves show linear stress–strain relationship immediately followed by brittle fracture. The tensile stress–strain curves for other types of syntactic foams also showed similar features [28, 29]. The tensile characteristic such as maximum tensile strength and tensile modulus shown in Figure 9 for details. The maximum tensile strength from overall specimens is belong to SCFT-01 at 38 MPa. However, it is led by pure vinyl ester at 40 MPa and for all specimens shows decreased when increased glass microballoon contents.

The tensile strength is observed is decreased to 20 MPa for SCFT-02. But then it was increased 5% for SCFT-03 to 25 MPa and decreased again for SCFT-04. While it is continued to reduce for SCFT-05 at 24 MPa

before it is fractured. Hence, there is no trend shows for tensile strength particularly when added with glass microballoon contents into the matrix resin as well. For the reduction of strength value of the syntactic foam are might be concerned with matrix phase in system which is act as load bearing phase as suggested by Wouterson *et al.* [30]. They tested glass microballoon in epoxy resin as matrix system. From their observation, it was found that matrix-microballoon interface does not appear to be very strong in these composites, and the presence of higher volume fraction of microballoons only reduces the volume fraction of epoxy resins in the structure, causing the lower strength of syntactic foams.

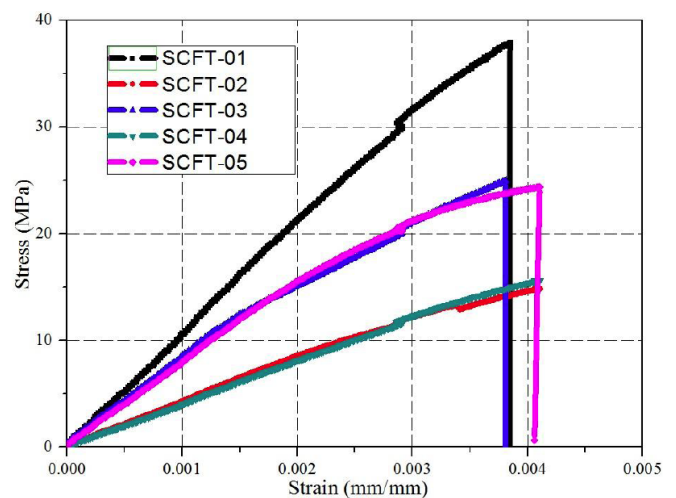


**Figure 8:** Overview representative tensile stress-strain curve for (a) SCFT-01 (b) SCFT-02 (c) SCFT-03 (d) SCFT-04 (e) SCFT-05.

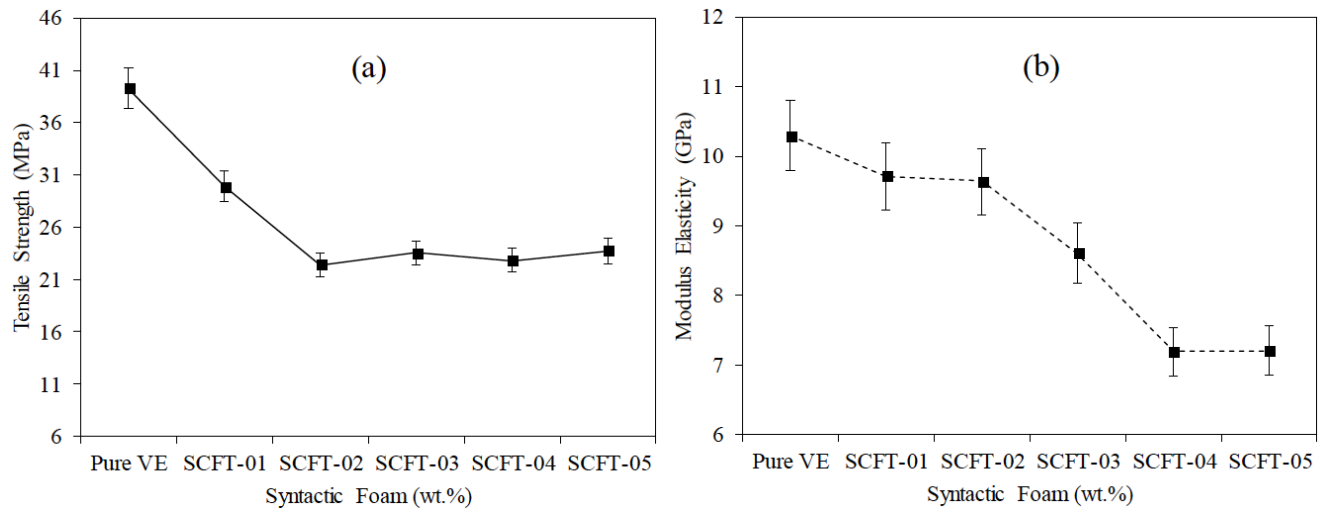


**Figure 9:** Graph for tensile properties syntactic foam (a) Modulus Elasticity (b).

Generally the modulus elasticity is decreased for all specimens except SCFT-02 which is higher modulus elasticity when compared with pure vinyl ester at 0.04 GPa. The ranging of modulus elasticity for all specimens between 0.03 to 0.04 GPa. While the specific tensile value also shows reduction when added more glass microballoon in the syntactic foam. It is clear that the increased of glass microballoon content can be effected particularly the matrix-glass microballoon interface bonding in these composite. Similar to Waterson *et al.* [30], the increased weight percentage of glass microballoon only reduced the volume fraction of vinyl ester. Therefore the strength of the composite was reduced when decreased the matrix contents.

The representative observation of fractured tensile for all specimens can be seen in Figure 10. It can be observed that the fractured specimens have been broken at within the extensometer range of 250mm in

length. The tensile fracture mechanism seems to be mainly related to particle–matrix debonding. The matrix propagation was occurred between matrix and glass microballoons and similar result was observed by Swetha and Kumar [31]. As a result, the majority of fractured pattern for all specimens were identified at narrow section bottom area except, SCFT-03 specimen which was occurred at near to the middle range of extensometer length. Therefore, with a decrease in the volume fraction of the matrix resin in the material structure, the strength of the composite is observed to be decreased. It is also shown that contributed to the low density behaviour if decreased the matrix contents in syntactic foam. It should be noted that the calculation of tensile stress and modulus elasticity values are based from the equations suggested in the corresponding standard.

The Poisson's ratio for all specimens can be determined by using the standard method according to

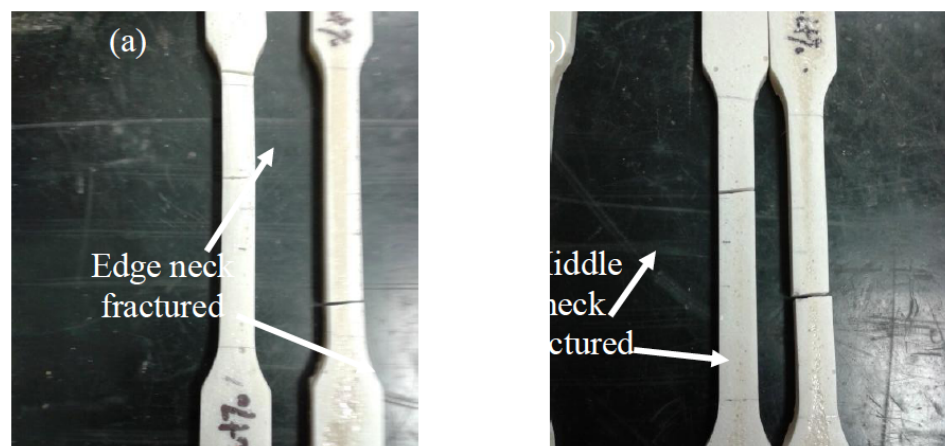


**Figure 10:** Typical of fractured tensile specimens (a) SCFT-02 (b) SCFT-03 after performed the testing.

**Table 1: Stress Concentration Factor Values Using FEA Method**

Specimens	Radius	Distance	Width	SCF, $K_{tm}$	SCF, $K_{te}$	Poisson's Ratio	Diff. ( $K_{tm} - K_{te}$ )
	r (mm)	h (mm)	$D_1$ (mm)	Modelling	Experimental	$\nu$	%
SCFT-01	28	58	20.0	1.95	1.73	0.38	11
SCFT-02	26	60	19.7	1.30	1.72	0.45	24
SCFT-03	28	60	19.8	1.37	1.71	0.37	20
SCFT-04	28	57	19.9	1.15	1.74	0.38	34
SCFT-05	28	60	19.7	1.57	1.70	0.46	8

the ASTM D-638. The Poisson's ratio value for all the specimen show in Table 1. The Poisson's ratio ( $\nu_{VE}$ ) and the Young's modulus ( $E_{VE}$ ) of neat vinyl ester resin specimens are measured as the first step. The value of  $\nu_{VE}$  is found to be 0.57, while  $E_{VE}$  is measured to be 11 GPa. This value is used to estimate the Poisson's ratio of various syntactic foam composites ( $\nu_c$ ) using a recent theoretical model, where the material properties of the microballoon glass material are taken as  $E_{MB}=60$  GPa and  $\nu_{MB}=0.21$  [32]. It shows that SCFT-02 has higher Poisson's ratio with 0.46 and minimum at 0.37 for SCFT-03 if compared with vinyl ester is still has higher value at 0.57. Generally, the Poisson's ratio is decreased while increasing the glass microballoon contents in the composite showed in Table 1. Similar to the previous worked, Wouterson *et al.* [30] was found the Poisson's ratio is varied from 0.30 to 0.35 in his study when added with nanoparticles.

### 3.2. Stress Concentration Factor (SCF) Analysis

The stress concentration factor was calculated according to the Equation (3) for all the specimens. Generally the SCF values are comparable with the SCF from modelling FEA by considering the maximum stress at the particular area and stress reference as 238 MPa. Starting from the SCF-01 with the composition of glass microballoon 2 wt.% has higher SCF,  $K_{ff}$  at 1.95. Table 1 shows the SCF values with the maximum stress distribution at four locations area on plate elements (GP1 to GP4).

From the Table 1 shows that the maximum stress also belongs to SCF-01 with 464 MPa which is matrix bonding of vinyl ester resin is higher than other specimens. This is cause of the calculation by using the Equation (3) was involved with the parameters such as radius (r) of curvature tensile and distance (h) are important to measure in this study. The maximum measurement for distance h is 60 mm while the maximum for radius r is 28 mm. Another parameter has involved for this SCF value is width of grip area for

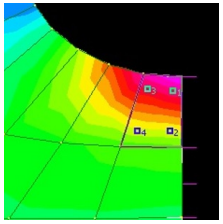
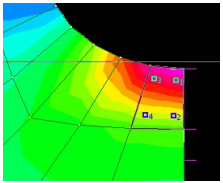
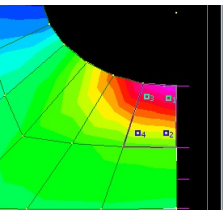
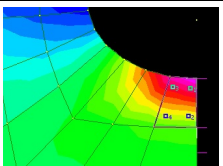
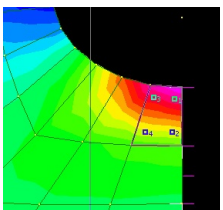
tensile specimen,  $D_1$  with maximum value 200 mm. The comparison between SCF for modelling and experimental also can be shown. Mbandezi and Mabuza use the formula maximum stress before refinement meshing and after refinement meshing to compute the numerical error percentage [33]. Numerical comparison also done by Collins between maximum normal stress in experimental and simulation [34]. In this study, the comparison between experimental and modelling was compute using the stress concentration factor method. From this graph, SCF experiment led the highest for SCFT-01 with difference 11 % when compared with SCF modelling. The SCF values for modelling is not much varied for all specimens while SCF for experiment show the trend is decreased when addition of glass microballoon in the composite accepted for SCFT-05. The percentage different between stress concentration factor  $K_{tm}$  and  $K_{te}$  showed that SCFT-05 has lower percentage with 8% error while SCFT-04 at maximum percentage with 34% error.

### 3.3. Stress Distribution from FEA

The stress concentration factor for all specimens which were analysed using the Strand 7 with the output results shown at Table 2. The contour pattern among all specimens showed the stress intensity area is focused on the narrow neck of tensile specimens. The plate property for each SCF can be determined from the Strand7 software at four point in the selected area as G1, G2, G3, G4 and centroid point. Table 2 shows all the related values for very each point in xy-direction with z-direction considered as zero because it occurred for 2D modelling. The centroid point was located at the middle cross between G1 to G2 and G3 to G4. In Strand7 the centroid is not appeared in the contour line but the value is given in tabulated data.

From the Table 2, it shows that the maximum stress also belong to SCF-01 with  $4.0390 \times 10^3$  MPaat centroid area. For other specimens from SCFT-02 to

**Table 2: Stress Distribution Values Using FEA Method**

Specimens	Centroid	G1	G2	G3	G4	Stress Distribution
	XY (10 <sup>3</sup> MPa)	Photo's				
SCFT-01	4.0390	4.8789	3.2846	4.7768	3.2156	
SCFT-02	2.4329	2.9557	1.9701	2.8820	1.9236	
SCFT-03	2.8287	3.4169	2.3004	3.3454	2.2520	
SCFT-04	2.3976	2.8961	1.9498	2.8355	1.9088	
SCFT-05	2.9510	3.5852	2.3897	3.4958	2.3333	

SCFT-05 the maximum stress is varied between 2.4 to 2.9 x 10<sup>3</sup> MPa. The results also show that the maximum stress distribution occurred at the plate element property no. 3. This result is confirmed with by referred the Figure 8 with a higher stress distribution particularly SCFT-01 because the matrix resin content is higher than other specimens due to plasticity. This is valid results by using the numerical modelling when determine their SCF individually.

#### 4. CONCLUSIONS

The finite element model using the Strand7 software was established to analyse the stress concentration factor (SCF) for different composition of glass microballoons in vinyl ester matrix resin syntactic foam.

Five compositions with different weight percentage were figured out using the formula SCF comparable between experimental and theoretical values. It was found that the both of SCF experimental and the theoretical values are varied but no trend shows among of them when the weight percentage of glass microballoons is increased in syntactic foam. From the results, it is showed that the SCF for experimental is not much different between 1.70 –1.74. While SCF for modelling more varied with minimum 1.15 and maximum is 1.95. It was occurred when increased the glass microballoon content in syntactic foam. It is also indicating that, the SCF is more sensitive to material with small modulus elasticity than the large modulus elasticity for the experimental SCF values. While it also

indicates that, the SCF is sensitive to the small Poisson's ratio than the large Poisson's ratio for the theoretical SCF values. Finally from the FEA Strand7 modelling, it shows that the stress distribution are varied with the different weight percentage (wt.%) of glass microballoons, which is higher values particularly for lower weight percentage of glass microballoons SCFT-01 specimen.

## ACKNOWLEDGEMENTS

The authors would like to thank Majlis Amanah Rakyat (MARA), Malaysia and Universiti Kuala Lumpur Malaysian Institute of Marine Engineering Technology, Malaysia for providing scholarship to the first author on doing this work.

## REFERENCES

- [1] Sburlati R, Atashipour S, Atashipour S. Reduction of the stress concentration factor in a homogeneous panel with hole by using a functionally graded layer. *Composites: Part B* 2014; 61: 99-109. <https://doi.org/10.1016/j.compositesb.2014.01.036>
- [2] Nagpal S, Jain N, Sayal S. Stress concentration and its mitigation techniques in flat plate with singularities: a critical review. *Eng Journal* 2012; 16(1): 1-16. <https://doi.org/10.4186/ej.2012.16.1.1>
- [3] Chao C, Lu L, Chen C, Chen F. Analytical solution for a reinforcement layer bonded to an elliptic hole under a remote uniform load. *Int Journal Solids Structure* 2009; 46: 2959-65. <https://doi.org/10.1016/j.ijsolstr.2009.03.025>
- [4] Batista M. On the stress concentration factor around a hole in an infinite plate subjected to a uniform load at infinity. *Int Journal Mechanics Science* 2011; 53(4): 254-61. <https://doi.org/10.1016/j.iimecs.2011.01.006>
- [5] Abdul-Aziz A, Abumeri G, Garg M, Young P. Structural Evaluation of a Nickel Base Super Alloy Metal Foam Via NDE and Finite Element. In: Monitoring SSSaMNEaH, editor. *Behavior and Mechanics of Multifunctional and Composite Materials II*, Conference SSN04; San Diego, California USA: SPIE; 9-13 March 2008. <https://doi.org/10.1117/12.776343>
- [6] Reale S, Tognarelli L, Crutzen S. The use of fracture mechanics methodologies for NDT results evaluation and comparison. *Nuclear Engineering and Design* 1995; 158: 397-407. [https://doi.org/10.1016/0029-5493\(95\)01046-K](https://doi.org/10.1016/0029-5493(95)01046-K)
- [7] Ingraffea A, Wawrzynek P. Computational Fracture Mechanics: A survey of the field. *European Congress on Computational Methods in Applied Sciences and Engineering*, ECCOMAS 2004. <https://doi.org/10.1002/0470091355.ecm032>
- [8] Poveda R, Gupta N, Porfiri M. Poisson's ratio of hollow particle filled composites. *Materials Letters* 2010; 64: 2360-2. <https://doi.org/10.1016/j.matlet.2010.07.063>
- [9] Gupta N, Woldesenbet E, Mensah P. Compression Properties of Syntactic Foams: Effect of Cenosphere Radius Ratio and Specimen Aspect Ratio. *Composites: Part A* 2004; 35: 103-11. <https://doi.org/10.1016/j.compositesa.2003.08.001>
- [10] Gladysz G, B BP, G GM, Lula J. Three-phase syntactic foams: structure property relationships. *Journal Material Science* 2006; 41: 4085-92. <https://doi.org/10.1007/s10853-006-7646-9>
- [11] Lin T, Gupta N, Talalayev A. Thermal conductivity of multiphase particulate composite materials. *Journal Material Science* 2009; 44: 1540-50. <https://doi.org/10.1007/s10853-008-3040-0>
- [12] Jain N, Mittal N. Finite element analysis for stress concentration and deflection in isotropic orthotropic and laminated composite plates with central circular hole under transverse static loading. *Material Science and Engineering, A* 2008; 498: 115-24. <https://doi.org/10.1016/j.msea.2008.04.078>
- [13] Gupta N, Woldesenbet E, Kishore, Sankaran S. Studies on Compressive Failure Features in Syntactic Foam Material. *Journals of Sandwich Structures and Materials* 2001; 4: 249-72. <https://doi.org/10.1177/1099636202004003140>
- [14] Islam MM, Kim HS. Novel syntactic foams made of ceramic hollow micro-spheres and starch: theory, structure and properties. *Journal of Materials Science* 2007; 42(15): 6123-32. <https://doi.org/10.1007/s10853-006-1091-7>
- [15] International A. *ASTM D 638-10 Standard Test Method for Tensile Properties of Plastics*. USA: ASTM International; 2010.
- [16] Warren C, Richard G. *Stress Concentration Factor*. Roark's Formula for Stress and Strain 7th edition ed. USA: Mc Graw-Hill; 2002. p. 784-5.
- [17] Strand7. *Introduction to the Strand7 Finite Element Analysis System*. 3rd edition ed. Sydney, Australia 2010.
- [18] Timoshenko S, Goodier J. *Theory of Elasticity*. Third Edition ed: McGraw-Hill, Inc; 1969.
- [19] Yang L, Zhu H, Tan D. Influence of Soft Filler on Stress Concentration Factor of Elliptic Holes in a Rectangular Plate. *Tianjin University and Springer-Verlag Berlin Heidelberg* 2012; 18: 117-20. <https://doi.org/10.1007/s12209-012-1614-z>
- [20] Shigley JE, Mischke CR, Budynas RG. *Mechanical Engineering Design*. New York USA: McGraw-Hill; 2004.
- [21] Adis J, Muminovic, Saric I, Repcic N. Analysis of Stress Concentration Factors using Different Computer Software Solutions. *Procedia Engineering* 2014; 69: 609-15. <https://doi.org/10.1016/j.proeng.2014.03.033>
- [22] Spotts MF, Shoup TE, Hornberger LE. *Design of Machine Elements*. 8th ed. New Jersey: Prentice Hall; 2004.
- [23] Darwish F, Tashtoush G, Gharaibeh M. Stress concentration analysis for countersunk rivet holes in orthotropic plates. *European Journal of Mechanics A/Solids* 2013; 37: 69-78. <https://doi.org/10.1016/j.euromechsol.2012.04.006>
- [24] Pilkey W, Pilkey D. *Peterson's Stress Concentration Factors*. 3rd ed. New York USA: John Wiley & Sons; 2008.
- [25] Shivakumar K, Newman J. Stress Concentrations for Straight-shank and Countersunk Holes in Plates Subjected to Tension, Bending, and Pin Loading. In: *National Aeronautics and Space Administration OoM, Scientific and Technical Information Program*, editor. NASA Technical Paper 1992.
- [26] Wu H, Mu B. On stress concentrations for isotropic/orthotropic plates and cylinders with a circular hole. *Composites: Part B* 2003; 34(2): 127-34. [https://doi.org/10.1016/S1359-8368\(02\)00097-5](https://doi.org/10.1016/S1359-8368(02)00097-5)
- [27] Kotousov A, Wang C. Three-dimensional stress constraint in an elastic plate with a notch. *International Journal of Solids and Structures* 2002; 77: 1665-81. [https://doi.org/10.1016/s0020-7683\(02\)00340-2](https://doi.org/10.1016/s0020-7683(02)00340-2)
- [28] Gupta N, Ye R, Porfiri M. Comparison of tensile and compressive characteristics of vinyl ester/glass microballoon syntactic foams. *Composites Part B: Engineering* 2010; 41(3): 236-45. <https://doi.org/10.1016/j.compositesb.2009.07.004>

- [29] Gupta N, Nagorny R. Tensile properties of glass microballoon-epoxy resin syntactic foams. *Journal of Applied Polymer Science* 2006; 102(2): 1254-61. <https://doi.org/10.1002/app.23548>
- [30] Wouterson EM, Boey FYC, Hu X, Wong SC. Effect of fiber reinforcement on the tensile, fracture and thermal properties of syntactic foam. *Polymer* 2007; 48: 3183-91. <https://doi.org/10.1016/j.polymer.2007.03.069>
- [31] Swetha C, Kumar R. Quasi-static uni-axial compression behaviour of hollow glass microspheres/epoxy based syntactic foams. *Materials & Design* 2011; 32(8-9): 4152-63. <https://doi.org/10.1016/j.matdes.2011.04.058>
- [32] Aureli M, Porfiri M, Gupta N. Effect of polydispersivity and porosity on the elastic properties of hollow particle filled composites. *Mechanic Materials* 2010; 42: 726-39. <https://doi.org/10.1016/j.mechmat.2010.05.002>
- [33] Mbandezi M, Mabuza R. The Effect of Variations of Crack Geometry on the Stress Concentration Factor in a Thin Plate Using Finite Element Method. 18th World Conference on Nondestructive Testing; Durban, South Africa 2010.
- [34] Collins J. Failure of materials in mechanical design analysis, prediction, prevention. 2nd ed. New York, USA: John Wiley & Sons, Inc., New York, USA; 1993.

Received on 17-10-2016

Accepted on 15-12-2016

Published on 06-04-2017

DOI: <https://doi.org/10.6000/1929-5995.2017.06.01.4>